14

Magnetic impedance of film nanostructures for stray magnetic field evaluation of microparticles in magnetic composites

© *G.Yu. Melnikov, V.N. Lepalovskij, G.V. Kurlyandskaya*

Ural Federal University after the first President of Russia B.N. Yeltsin,
20002 Yekaterinburg, Russia
e-mail: grisha2207@list.ru

Received September 17, 2021
Revised October 21, 2021
Accepted October 22, 2021

Longitudinal giant magnetoimpedance effect of $[Fe_{21}Ni_{79}/Cu]_5/Cu/[Fe_{21}Ni_{79}/Cu]_5$ film element was investigated depends on stray magnetic field of epoxy magnetic composite with 30% weight concentration of iron oxide magnetic microparticles. Configuration of an experiment was a model of thrombus detection in a blood vessel. Stray magnetic field was varied by movement of a magnetic composite above the element perpendicular to the long side. Composite was either magnetized or not to the state of remanence. As the magnetic composite approaches the GMI element, MI ratio curves are smoothed and shifted along the field axis and maximum value of the MI ratio decreases. Magnetic properties of magnetic composite and film element were investigated as well.

Keywords: Magnetoimpedance effect, multilayered film nanostructures, composite materials, biodetection.

DOI: 10.21883/TP.2022.02.52958.259-21

Introduction

Giant magnetoimpedance (GMI) is a phenomenon of change in ferromagnetic conductor impedance under the action of an external magnetic field when high-frequency current flows in it. This effect is characterized by high sensitivity in relation to the external magnetic field. Sensitivities up to 300%/Oe [1,2] have been obtained in multilayer film structures. Moreover, technologies for their making are compatible with methods for manufacture of semiconductor electronics components [3]. The FeNi permalloy satisfies the mandatory conditions for observing a significant magnetoimpedance effect: a high magnetic permeability, a low coercitive force and a possibility to generate uniaxial magnetic anisotropy [2–4]. GMI is due to a change in the skin depth of a ferromagnetic conductor upon application of a constant external magnetic field due to a change in effective magnetic permeability. Therefore, the thicker a magnetic film, the lower the frequencies at which a high GMI effect is observed [5]. However, with thicknesses of about 100 nm it changes into a „post-critical" state characterized by rotating anisotropy [6,7]. A transition to the „post-critical" state deteriorates the permalloy high-permeability properties (coercitive force increases, dynamic magnetic permeability and magnitude of GMI effect decrease). This problem can be solved by nanostructuring — separation of permalloy magnetic layers by interlayers of non-ferromagnetic or even magnetic conducting material of another type, thus forming a multi-layer structure [8–10].

One of the tasks solved using sensors of weak magnetic fields based on the GMI effect is the detection of stray magnetic fields that contain information about the object under study, e.g., positions of thrombi (pathological formations in the form of blood clots) in blood vessels. Nowadays treatment of thrombi is a complex therapeutic task related to the use of high thrombolytic doses that cause adverse events. The problem can be solved by using magnetic nanoparticles (MNP) for address delivery of thrombolytics directly to the therapeutic treatment area — to the thrombus zone. Magnetic nanoparticles carrying an active agent on their surface are be administered intravenously and delivered to the thrombus zone with the use of a gradient magnetic field. Diagnostic and therapeutic purposes require determination of their concentration near a thrombus; it can be done by estimating the magnitude and geometry of MNP stray fields [11,12]. The use of a GMI detector at this stage presupposes determination of the dependence of sensitive element impedance on stray magnetic fields taking into account their characteristics (direction, inhomogeneity, intensity etc.). At the initial research stage, filled composites of epoxy resin that contain magnetic particles are good model materials whose magnetic properties are rather close to those of real objects.

In this paper we have studied the magnetic properties of filled composites and a rectangular film GMI element $[Fe_{21}Ni_{79}/Cu]_5/Cu/[Fe_{21}Ni_{79}/Cu]_5$, and determined dependences of the GMI effect magnitude on peculiarities of stray magnetic fields of an epoxy resin composite in the form of a flat cylinder with 30% weight content of iron oxide microparticles in a model geometry that simulates the geometry of a thrombus in a blood vessel.

1. Measurement techniques and specimens

Multilayer film structures have been obtained by ion-plasma sputtering of an alloy target consisting of

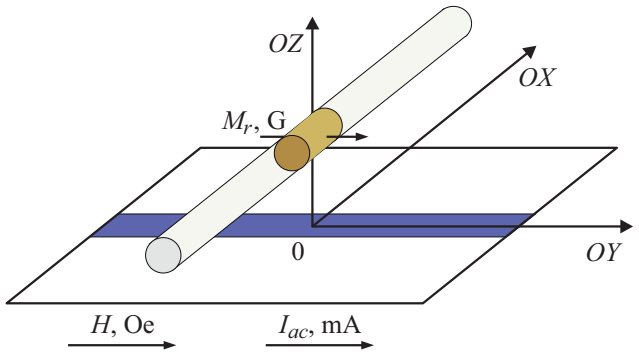

Figure 1. Layout of a model experiment for detection of stray fields of a magnetic composite that simulates a thrombus in a blood vessel.

$Fe_{20}Ni_{80}$ onto glass substrates. Sputtering was done through metal masks in a 100 Oe magnetic field to generate uniaxial magnetic anisotropy. The GMI elements had the dimensions of 10.0 ± 0.5 mm and the structure $[Fe_{21}Ni_{79}(100\,nm)/Cu(3\,nm)]_5/Cu(500\,nm)/[Fe_{21}Ni_{79}(100\,nm)/Cu(3\,nm)]_5$; an external field was applied along the element's short side in its plane. The fore vacuum was $3\cdot10^{-7}$ mbar, and the argon operating pressure was $3.8\cdot10^{-3}$ mbar. The composition of iron-nickel layers was clarified by means of energy dispersive X-ray analysis.

A model of a thrombus in a blood vessel was an epoxy resin cylinder placed in a polymer tube 5.1 mm in diameter, in the middle of which the epoxy resin composite with 30% weight content of commercial microparticles of FeO_x iron oxide was placed (the Fe_3O_4 phase — 94% wt.; Fe_2O_3 — 1% wt. and FeO(OH) — 5% wt.) (manufactured by Alfa Aesar (Ward Hill, MA, USA)). The composite had the shape of a flat cylinder having the diameter of 5.0 mm, length of 4.0 mm and weight of 0.1 g. The reference specimen (Reference) was an epoxy resin cylinder without magnetic particles. The average size of iron oxide microparticles was determined using the data of scanning electron microscopy (JEOL JSM-7000 F, Japan).

Epoxy-diphenylolpropane resin KDA (Chimex Ltd., Saint Petersburg, Russia) was used as a polymer matrix for the making of magnetic composite. The resin was first mixed with hardener — triethyl-tetraamine (Epital, Moscow, Russia) in the weight ratio of 6 : 1. Then weighed portions of powdered specimens were mixed with a liquid compound of epoxy resit at 25°C for 10 min to obtain a homogeneous mixture. The mixture was then placed in a cylindrical polyethylene form for hardening during 2 h at 70°C. The magnetic properties of the composite were studied using a 7407 VSM vibrating sample magnetometer (Lake Shore Cryotronics, USA) at room temperature. The film element's magnetic properties were studied using a magneto-optical Kerr microscope (Evico magnetics GmbH, Germany).

High-frequency impedance was measured using an Agilent HP E 4991 A impedance analyzer at room temperature in an external magnetic field generated by Helmholtz coils. The field was applied along the long side of GMI elements in the alternating current flow direction (a longitudinal configuration of GMI) in the field range of $H=-150-150$ Oe, interval of 0.33 Oe in the excitation current frequency range $I_{ac}(f)$, $f=1-400$ MHz.

The GMI-effect of film structures was studied in model experiments simulating a thrombus present in a blood vessel. Impedance was measured at different positions of the magnetic composite in relation to the film element. The composite was placed in the specimen at a distance of $(1.1-0.2)$ mm from the element surface and was moved perpendicularly to the long side of the GMI element. The position of the composite center from the film element center was counted along the Ox axis, the interval being 1 mm. The experiment was carried out in two variants: without magnetic biasing of the magnetic composite and with magnetic biasing up to the state of remanent magnetization $M_r=2.5$ G (Fig. 1). Magnetization direction matched the direction of the applied field. The GMI research results were described using a field dependence of magnetoimpedance ratio (MI): $\Delta Z/Z(H)=100\%\cdot(Z(H)-Z(H_{max}))/Z(H_{max}$, where $H_{max}=100$ Oe is the field where magnetic saturation of a film specimen occurs upon application of an external magnetic field along its long side. Hmax differs from the maximum external field used in the experiment.

The GMI response of an element in the presence of magnetic composite's stray fields was expressed as: $\Delta(\Delta Z/Z)=\Delta Z/Z_{control}-\Delta Z/Z_{position}$, where $\Delta Z/Z_{control}$ — MI ratio measured with the reference specimen; $\Delta-Z/Z_{position}$ — MI ratio measured with the composite in a certain position. The GMI frequency dependence was described using the maximum value of the MI ratio $\Delta Z/Z_{max}$ at a certain frequency. The random error was calculated on the basis of three measurements, using the Student's coefficient of 2.4 and confidence probability of 0.95. The relative systematic error did not exceed 1%.

2. Results and discussion

The epoxy resin magnetic composite containing 30% of magnetic parties has the saturation magnetization $M_s=29$ G, coercitive force $H_c=85$ Oe, remanent magnetization $M_r=2.5$ G. The magnetization curve shows that the magnetization of the composite was about 0.3 G in the field of the GMI element's maximum sensitivity of 4.1 Oe. The GMI effect is measured in the range of $H=-150-150$ Oe, but it is considered that reversible remagnetization takes place in the magnetic composite in the said field. Consequently, the given magnetization value can be taken as an estimate for the experimental study of the film element GMI effect in the presence of composite's stray fields, without its preliminary magnetization up to saturation (Fig. 2).

The magnetic hysteresis loops obtained using the Kerr microscope indicate the presence of induced magnetic anisotropy of the film element perpendicularly to its long

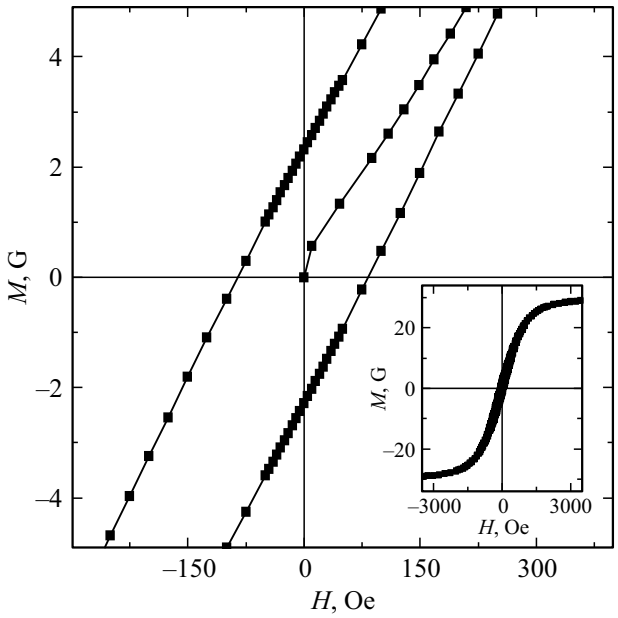

Figure 2. Magnetic hysteresis loop of the magnetic composite together with the initial magnetization curve.

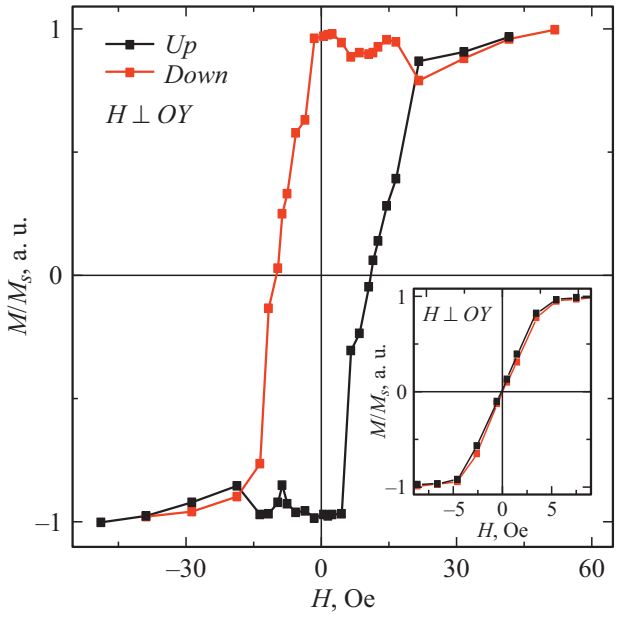

Figure 3. Magnetic hysteresis loop measured using the Kerr microscope in a magnetic field perpendicular to the long side of the GMI element. The insert shows: magnetic hysteresis loop measured in a field parallel to the long side of the GMI element.

side. Remagnetization along the long side is caused by rotation of the magnetization vectors (Fig. 3, insert), the anisotropy field is $H_a = 5$ Oe. Remagnetization perpendicularly to the long side is characterized by a rectangular hysteresis loop with coercitive force $H_c = 10$ Oe (Fig. 3).

The maximum value of the film element GMI ratio corresponds to the current frequency of 85 MHz (Fig. 4). The same current frequency corresponds to the maximum sensitivity of the GMI ratio to the external magnetic field of 41%/Oe in the 4.1 Oe field. MI ratio sensitivity depends on field magnitude, but there is a linear segment called the working interval ($H = 3.8-4.8$ Oe, $f = 85$ MHz) (Fig. 4), where it is constant and maximum.

The field dependence shows the GMI curves measured in descending and ascending external magnetic fields: from 150 Oe to −150 Oe (down), or −150 Oe to 150 Oe (up). The curves (up and down) for the given film element do not coincide at all the frequencies under study. A similar phenomenon has been observed earlier and it was explained, for instance, by a high sensitivity of the film structure to a transverse magnetic field in the vicinity of spin-reorientation phase transitions [13].

For simplicity, we will analyze only the downward branches from 150 Oe to −150 Oe (down), since the upward ones are symmetrical to them. The digits in the curves (Fig. 5, 6) specify the position of the magnetic composite center in relation to the GMI element center along the OX axis. The composite magnetization is $M = 0.3$ G in the experiments without preliminary magnetic biasing, near the field of the maximum sensitivity $H = 4.1$ Oe. When the composite approaches the GMI element, the maximum value of magnetoimpedance ratio decreases by approximately 2.5% in relation to the control (Fig. 5, insert).

Preliminary magnetization of the composite to the remanent magnetization $M = 2.5$ G results in the following: when the composite approaches the GMI element, the GMI ratio curves shift towards higher fields, and the maximum GMI ratio value decreases (Fig. 6). A shift of the curves is due to the influence of an additional component of stray fields along the long side of the GMI element (along the Y

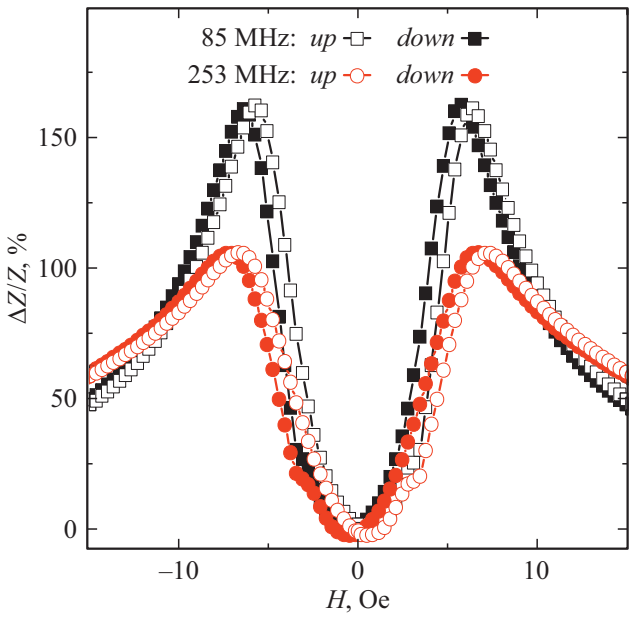

Figure 4. Field dependence of MI ratio at the frequencies of 85 and 253 MHz, downward branch (down) (from 150 to −150 Oe) and upward branch (up) (from −150 to 150 Oe).

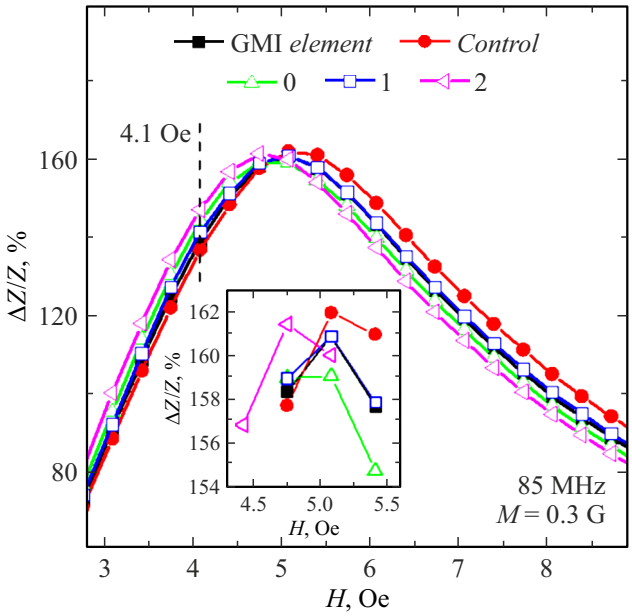

Figure 5. Field dependence of MI ratio at the frequency of 85 MHz with different positions of the magnetic composite with the magnetization of $M = 0.3$ G. The digits show the composite position in relation to the element in millimeters. The insert scale is enlarged.

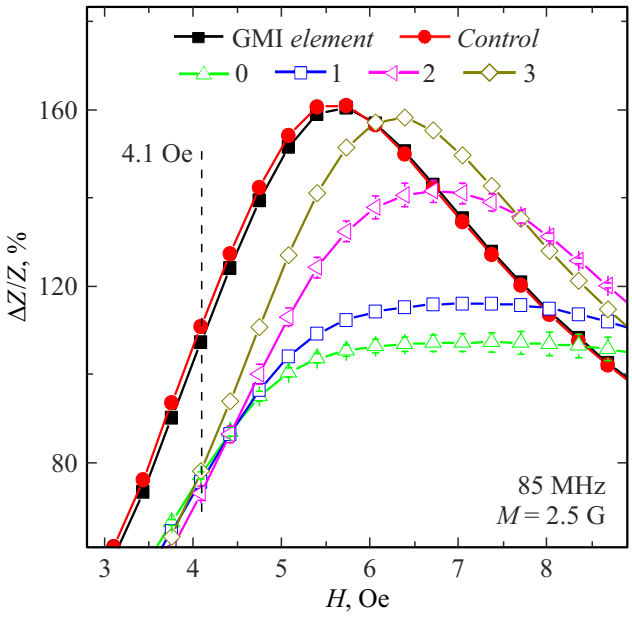

Figure 6. Field dependence of MI ratio at the frequency of 85 MHz with different positions of the magnetic composite with the magnetization of $M = 2.5$ G. The digits show the composite position in relation to the element in millimeters. MI ration for the GMI element only — (GMI-element); GMI element with control — (Control).

axis), while the transverse field component (along the X axis) can result in a decrease of the maximum MI ratio value [9]. It follows that the composite magnetization and the associated stray fields are not strictly oriented along the OY axis, but have components along the OX axis. This can be due to the fact that the magnetic composite has an effective axis of magnetic anisotropy.

It should be noted that one of the reasons of a change in the maximum GMI ratio value can be a change in permittivity of the composite base. For instance, it can be well seen in similar experiments with ferrogels having a high permittivity, where the maximum GMI ratio value greatly increases in non-filled gels [9]. In this paper, as was to be expected, permittivity of epoxy resin due to its smallness virtually does not affect the GMI effect: the GMI ratio curves, measured for a controlled GMI element (Control) and a non-controlled one (GMI element), coincide (Fig. 6).

In the experiment, position of the magnetic composite (with its magnetization $M = 2.5$ G) is detected well on the basis of the maximum GMI ratio (Fig. 7). The maximum GMI response is observed when the cylinder center is above the GMI element. The GMI response is much weaker when $M = 0.3$ G, but the same trend is observed (Fig. 7, insert). Some symmetrical positions of the magnetic cylinder (e.g., -2 and 2 mm) correspond to different values of the GMI ratio. This can be accounted for by certain inhomogeneity of the composite. The GMI response is almost zero for the positions of -4 and 4 mm, when the composite is wholly outside the film element.

When considering the response in the magnetic field of the maximum sensitivity (4.1 Oe, the dashed lines in Fig. 5 and 6) at $M = 2.5$ G, we can note that the extreme positions (-4 and 4 mm) correspond to the GMI response of about 30%, which means that the film element in this case is sensitive to stray magnetic fields at such a

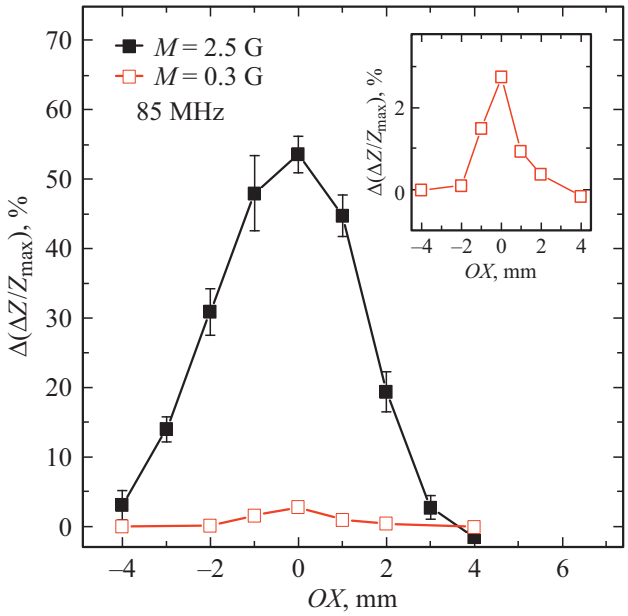

Figure 7. GMI response depending on magnetic composite position along the maximum MI ratio value according to the frequency of 85 MHz. The insert scale is enlarged.

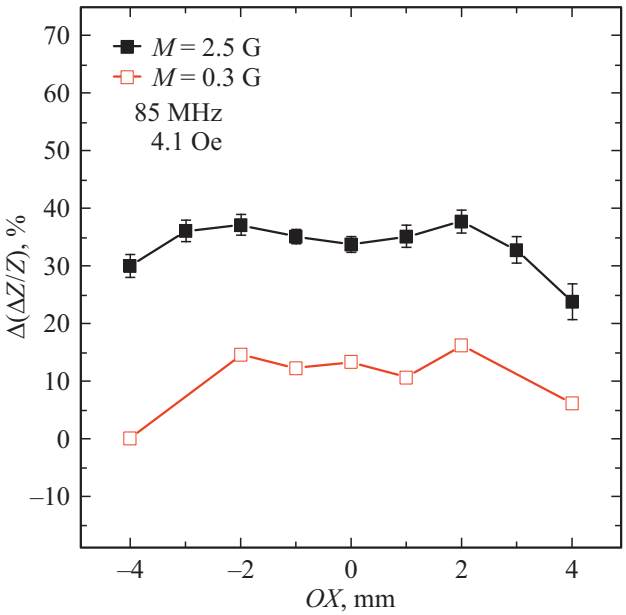

Figure 8. GMI response depending on magnetic composite position in the field of the maximum sensitivity of 4.1 Oe at 85 MHz.

distance. However, upon further approach the response hardly changes, the cylinder center corresponds to the local minimum (Fig. 8). Such behavior can be due to the fact that stray fields shift the operating point from the 4.1 Oe field to a region of lower sensitivity. The second reason is the decrease of the maximum GMI ratio value, resulting in decreased sensitivity. Though a close trend is observed at $M = 0.3$ G, the GMI response, depending on position, varies considerably less while the measurement error is much higher due to the complexity of detection of very weak signals.

The considered configuration is a simple model of positioning of a thrombus in a blood vessel, it gives a good idea of stray field impact on the GMI effect magnitude in this case and confirms the viability of works in the given area.

Conclusion

In the paper we have studied the magnetic properties and peculiarities of the longitudinal giant magnetoimpedance effect of a film element $[Fe_{21}Ni_{79}/Cu]_5/Cu/[Fe_{21}Ni_{79}/Cu]_5$ both in the presence of stray fields of iron oxide microparticles within the composite and without them in the model configuration of the experiment for thrombus detection in a blood vessel. The magnetic composite was epoxy resin with 30% weight content of magnetic particles.

An increase in stray magnetic fields upon approach of the composite to the GMI element causes a shift of the GMI ratio curves towards the higher-field region and a decrease of the maximum GMI ratio value. Supposedly, the shift is caused by the magnetic field component along the long side of the GMI element, while the transverse component causes a decrease in the maximum GMI ratio value. The change in the value of the maximum GMI ratio has allowed for detecting the magnetic cylinder position: the maximum response corresponded to the composite center above the GMI element. Detection was less efficient in the field of the maximum GMI element sensitivity. The possible reasons are:

1) the longitudinal component of stray fields shifts the operating point to a region of lower sensitivity;

2) the transverse component of stray fields reduces sensitivity by reducing the maximum GMI ratio value.

Conflict of interest

The authors declare that they have no conflict of interest.

References

[1] M.A. Correa, F. Bohn, C. Chesman, R.B. da Silva, A.D.C. Viegas, R.L. Sommer. J. Phys. D Appl. Phys., **43**, 295004 (2010). DOI:10.1088/0022-3727/43/29/295004
[2] A. García-Arribas, E. Fernández, A.V. Svalov, G.V. Kurlyandskaya, J.M. Barandiaran. J. Magn. Magn. Mater., **400**, 321 (2016). DOI:10.1016/j.jmmm.2015.07.107
[3] P. Ripka, K. Zaveta. *Magnetic Sensors: Principles and Applications*. In Handbook of Magnetic Materials (Elsevier, Amsterdam, The Netherlands, 2009), DOI:10.1016/S1567-2719(09)01803-4
[4] L.V. Panina, K. Mohri. Sensors and Actuators A: Physical, **81** (1–3), 71 (2000). DOI: 10.1016/S0924-4247(99)00089-8
[5] A.S. Antonov, S.N. Gadetsky, A.B. Granovsky, A.L. Dyachkov, V.P. Paramonov, N.S. Perov, A.F. Prokoshin, N.A. Usov, A.N. Lagarkov. FMM, **83**, 60 (1997) (in Russian).
[6] S. Tikadzumi. *Magnitnye kharakteristiki i prakticheskoye primeneniye* (Mir, M., 1987) (in Russian)
[7] P.R. Kern, O.E. da Silva, J.V. de Siqueira, R.D. Della Pace, J.N. Rigue, M. Carara. J. Magn. Magn. Mater., **419**, 456 (2016). DOI:10.1016/j.jmmm.2016.06.061
[8] M.S. Marques, T.J.A. Mori, L.F. Schelp, C. Chesman, F. Bohn, M.A. Corrâ. Thin Solid Films, **520** (6), 2173 (2012). DOI:10.1016/j.tsf.2011.10.028
[9] F.A. Blyakhman, E.B. Makarova, F.A. Fadeyev, D.V. Lugovets, A.P. Safronov, P.A. Shabadrov, T.F. Shklyar, G.Yu. Melnikov, I. Orue, G.V. Kurlyandskaya. Sensors, **18**, 872 (2018). DOI: 10.3390/s18030872
[10] N.A. Buznikov, A.S. Antonov. J. Superconduc. Novel Magnetism, **30** (9), 2569 (2017). DOI:10.1007/s10948-017-4069-6
[11] Q.A. Pankhurst, J. Connolly, S.K. Jones, J. Dobson. J. Physics D: Appl. Phys., **36**, R167 (2003). DOI: 10.1088/0022-3727/36/13/201
[12] A.Y. Prilepskii, A.F. Fakhardo, A.S. Drozdov, V.V. Vinogradov, I.P. Dudanov, A.A. Shtil, P.P. Bel'tyukov, A.M. Shibeko, E.M. Koltsova, D.Y. Nechipurenko, V.V. Vinogradov. ACS Appl. Mater. Interfaces, **10**, 36764 (2018). DOI 10.1021/acsami.8b02441
[13] G.V. Kurlyandskaya, N.G. Bebenin, V.O. Vas'kovsky. Phys. Metal. Metallogr., **111**, 133 (2011). DOI: 10.1134/S0031918X11010200